# Bridge Cracks Monitoring: Detection, Measurement, and Comparison using Augmented Reality

**Project No. 20STUNM33**

**Lead University: University of New Mexico**

**Final Report**

**August 2021**

# TECHNICAL DOCUMENTATION PAGE

| 1. Project No.<br>20STUNM33 | 2. Government Accession No. | 3. Recipient's Catalog No. | |
|---|---|---|---|
| 4. Title and Subtitle<br><br>**Bridge Cracks Monitoring: Detection, Measurement, and Comparison using Augmented Reality** | | 5. Report Date<br>August. 2021 | |
| | | 6. Performing Organization Code | |
| 7. Author(s)<br>PI: Fernando Moreu https://orcid.org/0000-0002-7105-7843<br>GRA: Kaveh Malek https://orcid.org/0000-0001-9009-2540 | | 8. Performing Organization Report No. | |
| 9. Performing Organization Name and Address<br><br>Transportation Consortium of South-Central States (Tran-SET)<br><br>University Transportation Center for Region 6<br>3319 Patrick F. Taylor Hall, Louisiana State University, Baton Rouge, LA 70803 | | 10. Work Unit No. (TRAIS) | |
| | | 11. Contract or Grant No.<br>69A3551747106 | |
| 12. Sponsoring Agency Name and Address<br><br>United States of America<br>Department of Transportation<br>Research and Innovative Technology Administration | | 13. Type of Report and Period Covered<br>Final Research Report<br>August 2020 – August 2021 | |
| | | 14. Sponsoring Agency Code | |

**16. Abstract**

Crack occurrence and propagation are among critical factors that affect the performance and lifespan of civil infrastructures such as bridges. Consequently, numerous crack detection and measurement methods have been proposed and developed in the recent decades in the areas of Structural Health Monitoring and non-destructive testing. Many novel technologies have emerged with the potential to overcome the limitations of the presented techniques of crack detection and characterization. Crack detection and characterization method used in this research lies in supplementing human visual inspection capabilities in a systematic manner through an appropriate level of automation. The Augmented Reality (AR) tool developed in this project allows a user to perform tasks in a real-world environment while visually receiving supplementary 3D computer-generated information to support the tasks. More specifically, we developed a crack detection/characterization tool in this research and deployed it in Microsoft HoloLens smart glasses. This AR tool provides the user with automatic data collection capability through AR headset camera and is a means of hands-free data sharing for inspectors while conducting their normal inspection. We conducted several laboratory and field experiments by which we evaluated the effectiveness of the developed crack detection and measurement system. The result confirm that the AR tool devised in this project has the potential to help the inspection process in terms of time, comfort and accuracy.

| 17. Key Words<br><br>Augmented Reality, Crack Detection, Pattern Recognition, Image Processing, Canny Algorithm. | 18. Distribution Statement<br><br>No restrictions. This document is available through the National Technical Information Service, Springfield, VA 22161. | | |
|---|---|---|---|
| **19. Security Classif. (of this report)**<br>Unclassified | **20. Security Classif. (of this page)**<br>Unclassified | **21. No. of Pages**<br>34 | **22. Price** |

**Form DOT F 1700.7 (8-72)**          **Reproduction of completed page authorized.**

# SI* (MODERN METRIC) CONVERSION FACTORS

## APPROXIMATE CONVERSIONS TO SI UNITS

| Symbol | When You Know | Multiply By | To Find | Symbol |
|---|---|---|---|---|
| **LENGTH** | | | | |
| in | inches | 25.4 | millimeters | mm |
| ft | feet | 0.305 | meters | m |
| yd | yards | 0.914 | meters | m |
| mi | miles | 1.61 | kilometers | km |
| **AREA** | | | | |
| $in^2$ | square inches | 645.2 | square millimeters | $mm^2$ |
| $ft^2$ | square feet | 0.093 | square meters | $m^2$ |
| $yd^2$ | square yard | 0.836 | square meters | $m^2$ |
| ac | acres | 0.405 | hectares | ha |
| $mi^2$ | square miles | 2.59 | square kilometers | $km^2$ |
| **VOLUME** | | | | |
| fl oz | fluid ounces | 29.57 | milliliters | mL |
| gal | gallons | 3.785 | liters | L |
| $ft^3$ | cubic feet | 0.028 | cubic meters | $m^3$ |
| $yd^3$ | cubic yards | 0.765 | cubic meters | $m^3$ |
| NOTE: volumes greater than 1000 L shall be shown in $m^3$ | | | | |
| **MASS** | | | | |
| oz | ounces | 28.35 | grams | g |
| lb | pounds | 0.454 | kilograms | kg |
| T | short tons (2000 lb) | 0.907 | megagrams (or "metric ton") | Mg (or "t") |
| **TEMPERATURE (exact degrees)** | | | | |
| $^oF$ | Fahrenheit | 5 (F-32)/9 or (F-32)/1.8 | Celsius | $^oC$ |
| **ILLUMINATION** | | | | |
| fc | foot-candles | 10.76 | lux | lx |
| fl | foot-Lamberts | 3.426 | candela/$m^2$ | $cd/m^2$ |
| **FORCE and PRESSURE or STRESS** | | | | |
| lbf | poundforce | 4.45 | newtons | N |
| $lbf/in^2$ | poundforce per square inch | 6.89 | kilopascals | kPa |

## APPROXIMATE CONVERSIONS FROM SI UNITS

| Symbol | When You Know | Multiply By | To Find | Symbol |
|---|---|---|---|---|
| **LENGTH** | | | | |
| mm | millimeters | 0.039 | inches | in |
| m | meters | 3.28 | feet | ft |
| m | meters | 1.09 | yards | yd |
| km | kilometers | 0.621 | miles | mi |
| **AREA** | | | | |
| $mm^2$ | square millimeters | 0.0016 | square inches | $in^2$ |
| $m^2$ | square meters | 10.764 | square feet | $ft^2$ |
| $m^2$ | square meters | 1.195 | square yards | $yd^2$ |
| ha | hectares | 2.47 | acres | ac |
| $km^2$ | square kilometers | 0.386 | square miles | $mi^2$ |
| **VOLUME** | | | | |
| mL | milliliters | 0.034 | fluid ounces | fl oz |
| L | liters | 0.264 | gallons | gal |
| $m^3$ | cubic meters | 35.314 | cubic feet | $ft^3$ |
| $m^3$ | cubic meters | 1.307 | cubic yards | $yd^3$ |
| **MASS** | | | | |
| g | grams | 0.035 | ounces | oz |
| kg | kilograms | 2.202 | pounds | lb |
| Mg (or "t") | megagrams (or "metric ton") | 1.103 | short tons (2000 lb) | T |
| **TEMPERATURE (exact degrees)** | | | | |
| $^oC$ | Celsius | 1.8C+32 | Fahrenheit | $^oF$ |
| **ILLUMINATION** | | | | |
| lx | lux | 0.0929 | foot-candles | fc |
| $cd/m^2$ | candela/$m^2$ | 0.2919 | foot-Lamberts | fl |
| **FORCE and PRESSURE or STRESS** | | | | |
| N | newtons | 0.225 | poundforce | lbf |
| kPa | kilopascals | 0.145 | poundforce per square inch | $lbf/in^2$ |

# TABLE OF CONTENTS

# LIST OF FIGURES

# LIST OF TABLES

## ACRONYMS, ABBREVIATIONS, AND SYMBOLS

AR   Augmented Reality

ARSG  Augmented Reality Smart Glasses

CN   Canadian National Railway

HMD  Head Mounted Device

LAC   Los Alamos County

MR   Mixed Reality

MRHMD Mixed Reality Head Mounted Device

NMDOT New Mexico Department of Transportation

SHM  Structural Health Monitoring

USDOT United States Department of Transportation

VR   Virtual Reality

# EXECUTIVE SUMMARY

It is a vital necessity to ensure appropriate and reliable functioning of infrastructure. The problem of infrastructure deterioration, in particular the decay of bridges has been noted by the State Departments of Transportation. The general score of bridge decay was D+ on the infrastructure report card from 2017, which has led the State Departments of Transportation in New Mexico to take steps to prevent further deterioration. Considering the budget limitation for infrastructure repair and maintenance, it is assumed that the most workable method to control the decay of infrastructure is to perform frequent, thorough, and objective inspections. Once routine inspections are performed over a period of time, infrastructure managers can compare their results and detect changes in the bridge condition. In consequence, infrastructure managers are able to prioritize bridge management plans so as to pay more direct attention to bridges and other elements of infrastructure that display more evidence of decay. Therefore, it is crucial to perform regular and thorough bridge inspections, as they play a pivotal role in determining the condition, and urgency of repair of the inventory of bridges in the state of New Mexico, ensuring the safety and security of bridge users. Accurate and reliable data collection by bridge inspectors remains a challenge. Some of the main challenges faced by bridge inspectors in the field include the following: (1) the insufficient amount of information that can be collected during the limited inspection time; (2) the variability of the data that is collected in between inspections, as even the same inspector may introduce some changes in between inspections in different years; and (3) the access and assimilation of past inspections while conducting the inspection at the bridge. To address the aforementioned problems, this project developed practical research solutions that can be adopted by the New Mexico Department of Transportation (NMDOT) in the future, the main contributions.

In this project we developed a new approach that made use of updated camera technologies and AR tools to explore the potential of a real-time crack sensing. We implemented the method of applying AR headsets such as HoloLens from Microsoft to enhance the amount of information that must be received by inspectors during crack detection. The headsets can be used during the video recording of observed damage, and the received images will be processed in real time, with the HoloLens computing capabilities. By using the HoloLens, the inspectors will be able to detect cracks that cannot be detected easily in real time otherwise. This solution, in turn, may provide the inspectors with an estimate damage assessment and damage prognosis of the structure under investigation. This approach can be implemented by the deployment of an image processing and data collection application in smart glasses. Users of the application can carry out hands-free on-site visual inspection, while visually receiving computer-generated information and collecting the inspection data from the site in real-time. More specifically, we developed a crack detection/characterization tool in this research and deployed it in Microsoft HoloLens smart glasses. The system can automatically take and save the picture of structures and mark the crack edges by a noticeable color (e.g. red) in the image and show it to the user. In addition, the dimensional characteristics of cracks can be instantly measured and shown to the inspectors in a real-time. The detection and measurement algorithms involve enhancement of images with a smoothing filter, finding and marking the edges of cracks using pattern recognition algorithm, and measuring the pixels placed between two edges of cracks by which the tool calculates the crack width.

The results of laboratory and field experiments, performed in the present study demonstrated the overall effectiveness of the AR tool developed in this project. For example, the experimental results showed that almost 75 percent of the length of tested cracks were normally detected and were shown to the inspector during the experiments. Having said that, the proposed AR methodology is real-time and semi-automatic, and therefore we consider the inspector will be able to notice a crack when the app shows the major portion of it to them. Then the human inspector can make their professional judgment on the cracked structure based on the dimensional characteristic that the crack measurement app provide for them. In addition, the results of measurement experiments in laboratory and field shows that the tool is able to measure the width of cracks with a reasonable accuracy. The maximum error for the width measurement in field and laboratory experiments are 16.7 and 13.3, respectively.

# 1. INTRODUCTION

Despite its critical role in driving the economy and improving the quality of life, existing infrastructure in the United States is deteriorating. Infrastructure systems in the USA, are subject to increasing demand due to higher transportation loads. Moreover, the infrastructure components deteriorate due to natural processes such as aging and the gradual wear and tear that comes with excessive utilization. It is expected that the deterioration may accelerate due to climate change, which may in turn lead to more frequent sudden environmental events, such as hurricanes and floods.

Given the limited funds that can be allocated to infrastructure repair and maintenance, performing inspection, which is defined as the evaluation of the physical and functional conditions of civil infrastructure systems, can be considered the most practical method to control the decay of infrastructure (1). This process, which is primarily vision-based, involves detection of any visual changes, such as leakages, cracks and corrosion, in these structures over the course of time (2). The importance of visual inspection in infrastructure repair and maintenance is frequently reported in the literature. For example, visual inspection techniques are the primary methods used to evaluate the condition of the majority of the nation's highway bridges and these subjective assessments may have a significant impact on the safety and maintenance of a bridge (3). Additionally, the rail inspection is one of the most important tasks to guarantee the safety of a railway transportation system (4).

Cracks, especially fatigue cracks are a frequent type of damage that affects infrastructure. Fatigue cracks occur because of repetitive service loads in civil structures, such as old steel highway bridges in the USA (5). The cracks are problematic and difficult to observe because they expand slowly, and it may take a long time, spanning to decades, until they achieve critical dimensions. It has been observed in the literature that the visual inspections are labor intensive, costly, and most of all, unreliable (6). For instance, past studies show that only 2% to 7% of the inspectors are able to detect target fatigue cracks correctly (7). This is because early fatigue cracks form very small openings, and the visual contrast between the crack and the adjacent surface is very low.

Nominal limit value of the crack width specified for concrete structure with expected functional consequences of cracking is given in national codes and international standards such as ISO 4179, (2005) and ACI 201 (2008) (8) and (9). In addition, stress intensity factor of the cracks is proportionate with the square root of crack size based on conventional fracture mechanism theories available in the mechanics of material text books (10). Therefore, measurement of crack width and size are of utmost importance in fracture mechanism of concrete.

Studies on crack detection and characterization actively and rapidly evolved in the last decade, and many novel technologies have emerged with the potential to overcome the limitations of the presented techniques. Two conventional branch of contacting crack detection technologies are direct sensing (such as discrete strain monitoring, distributed strain monitoring and direct sensing based on wave monitoring) and indirect monitoring (such as model-based approaches and model-free approaches). In addition, emerging technologies including wireless sensors, MEMS, thin-film and piezoelectric paints, nano-technologies, LAE, and noncontact sensing techniques, have introduced, recently (11).

However, all of the detection methods mentioned above are either quasi-real-time or non-real-time. Also, as far as the authors are aware of, the crack measurement through conventional image

processing methods are not simultaneously performed during the inspection. Crack detection and characterization method used in this research lies in supplementing human visual inspection capabilities in a systematic manner through an appropriate level of automation. The AR tool used in this project allows a user to perform tasks in a real-world environment while visually receiving Supplementary 3D computer-generated information to support the tasks.

The use of AR headset for crack detection and characterization was employed the previous studies such as (12) and (13). However, both studies used Artificial Neural Network based classification models for crack recognition that is different from pattern recognition algorithm employed in this project. Furthermore, those models were deployed on the headsets other than Microsoft HoloLens used in the present project that are connected to other processing device and use external processor for image processing.

In section 4, we introduce our proposed assisting system and the AR app in detail, and talk about the required hardware for the tool and its capabilities. In section 5 we present several experimental tests that were made to evaluate the tool in terms of accuracy of measurements, speed of inspection, and the comfort of the users. The experiments presented in section 5 involve the laboratory experimental tests performed on the images of cracks and the field tests carried out on the real cracks at different locations in the state of New Mexico. In these field tests, we used real concrete cracks to shows the performance of the tool for real crack detection and measurement. In addition, this section evaluates the influence of effective parameters on detection and measurement ability of the tool. Finally, some conclusions are offered in section 6.

## 2. OBJECTIVES

The new AR application will compare the bridge inspector capability to measure crack widths during inspections with and without AR.

## 2.1. Research Phase

The technical objectives of this research proposal include the following aspects:

i.   **Crack measurement AR design**. Contact LAC, CN, NMDOT, and collect their needs and suggestions for the use of AR for transportation infrastructure inspections. The research team wanted to determine, following NMDOT's assistance and advice, the current methods used by bridge inspectors to measure cracks in the field. Researchers used this information to perform post-processing of bridge images by comparing the cloud of point of the images over time through overlapping. The overlap of two or more images with different crack openings from different perspectives was used to realize a crack into a single coordinated system. The received images are used to assess the damage caused by the cracks, to evaluate the overall safety condition of the structure, and to prognose the future health monitoring plan. The researchers planed that the application of AR headsets would increase the inspectors' awareness of the crack damage and that was the main objective in the design of the AR application. With this objective, the inspectors who could potentially miss the crack damage if they would not obtain sufficient information during the observation, now they would see it in AR on real time, and that was of value according to the industry partners interviewed in this first objective. Moreover, all the information about the detected cracks wanted to be stored in a database that could help the inspectors who monitor the cracks later to see the previous state of the crack and to determine how it differs from the current crack. In this objective the research team became aware of the current limitations of the measurement systems that have been implemented to date as well as of the challenges that have been reported by the inspectors. Based on the information received, the research team plan to compile a summary of the current methods that are applied for crack detection, and accordingly, take further research steps planned to be undertaken.

ii.  **Laboratory crack measurement design and proof of concept.** In collaboration with LANL, the second objective was to elaborate a pilot research program to develop the various applications that can be benchmarked with LAC, CN, and NMDOT. The main purpose of the pilot program in this objective would be to establish the methodology used for testing and validation in laboratory settings. Specifically, the pilot research program needed to be developed in collaboration with the NMDOT bridge department to establish validation methodologies in the following:

     1.   Speed of inspection

     2.   Accuracy of inspection

     3.   User feedback

     Furthermore, the research team planned to design a laboratory experiment in this 2$^{nd}$ objective, whose purpose will be to measure crack widths with the application of AR tools such as HoloLens. It was expected that the outcome of the experiment would produce a preliminary selection of computer vision methods that could be implemented to measure

crack width. Subsequently, the research team wanted to develop software to integrate crack width sensing with AR tools. The research team then could demonstrate the experiment to NMDOT and request feedback. A preliminary set of specifications then could be made with NMDOT.

iii. **Crack field sensing using AR**: the research team then planned to design a new AR application with LAC, CN, and NMDOT for field measurements. This part relates to (ii) and will be part of the experiment performed with NMDOT. The research team planned to request NMDOT to select one bridge of their interest that could be used to test the proposed method in outdoors settings. Given to COVID, we developed the testing in the UNM campus, and we plan to do a field sensing in real bridges in the implementation phase. The results of the test were to be analyzed and written down, with a focus on the limitations of the new method and potential ways to overcome them. As a follow-up of the outdoors test, AR crack inspection specifications were updated. On the basis of the received feedback, the research team intended to determine an AR crack inspection specification with NMDOT.

iv. **Involve both students and industry** in (iii) The student involvement part included teaching the first class on AR for Transportation Infrastructure Inspections in UNM for high school students at the STI, which was originally an objective that was transformed in a summer internship for undergraduate students. We also set up of a webinar with Universities, National Laboratories, stakeholders, to summarize the achievements and receive feedback. An updated set of specifications was planned to be made with NMDOT to be sure that the outcome has an implementation in industry. Furthermore, we planned to work together with NMDOT in a nationwide AR implementation idea and that was achieved in the project, and currently is being improved with more feedback from NMDOT.

v. **Publications, presentations, and seminars** towards the dissemination of the development of AR for crack measurement using 3D cameras for field implementations, based on industry needs.

## 2.2. Implementation Phase

The results of this research will be tested by infrastructure owners because they have already expressed their interest by committing resources to the preliminary stages of using AR for inspection of transportation infrastructure (LAC, CN). The following implementation steps will be followed:

i. **Benchmarking of the results of using this software with conventional inspections** (field implementation). This will lead to the creation of a template with an AR crack inspection specification procedure, to be used by NMDOT, as well as a final report for TranSET.

ii. **Teaching of AR to high school students**, and undergraduate students with STEM classes. In addition, outreach activities on infrastructure management and maintenance involving students will be held.

iii. **Report to a panel review** composed on experts on AR, bridge inspection, railroad bridge maintenance, and human factors to receive feedback in the technology developed as well as the opportunities for industry implementation that can be overcome with AR.

iv. **Demonstration** at **international conferences** including the annual transportation research board (TRB) meeting in Washington, D.C. and the international workshop on structural health monitoring (IWSHM) in Stanford, California. A new workshop on AR will be provided with the International Modal Analysis Conference (IMAC) for using AR for bridge inspections.

# 3. LITERATURE REVIEW

## 3.1. Crack Identification Background Studies

In recent years, there has been an increasing interest in developing new technologies for crack detection and characterization in structural inspection. Two conventional branch of contacting crack detection technologies are direct sensing (such as discrete strain monitoring, distributed strain monitoring and direct sensing based on wave monitoring) and indirect monitoring (such as model-based approaches and model-free approaches). In addition, emerging technologies including wireless sensors, MEMS, thin-film and piezoelectric paints, nano-technologies, LAE, and noncontact sensing techniques, have introduced, recently (11).

Recently, a contactless, non-invasive, and non-destructive method is proposed for crack detection (14). They have used the thermal camera for detecting the reflection of an IR source from the surface of the crack. The proposed system uses the specular reflection to identify the presence of any crack defects. Then they isolate the crack based on the position and the geometry of the reference surface. They have their results similar to that of the rapid real-time data acquisition. Another research has proposed a new laser excited thermography technique with using laser spot array source (15).

Automatic inspection systems for crack characterization using image-based techniques have attracted increasing attention. In general, an inspection system includes two parts: defect detection devices and defect recognition algorithms. Recently, with the development of high-quality image acquisition devices and vision-sensing technologies, many advanced imaging technologies have been applied to the visual inspection of structures for example unmanned aerial vehicles and mobile robots with high-resolution cameras (16). These acquisition devices have greatly promoted the development of defect detection methods and the reliability of visual assessment. Lining cracks are a common and serious type of tunnel disease (17) that reflect the condition of the lining structure and may lead to concrete spalling, seepage, freezing damage, and other problems (17). To investigate such problems, researchers have developed novel mobile inspection machines to identify tunnel-lining cracks. Yu introduced a mobile image acquisition system to scan tunnel-linings consisting of a mobile robot and a charge coupled device (CCD) camera that uses velocity sensors and shock-absorbing devices to control the line CCD camera and obtain fine-grained crack images (18). Menendez presented a multiple-degrees-of-freedom robot consisting of a mobile vehicle, an extended crane and a high precision robotic arm with a 3D vision system and ultrasonic sensors mounted on the front to detect crack features (19).

An image stitching algorithm has been adopted which works on feature based registration by using skeletonization algorithm for the retrieval of the crack segments (20). The detection of the crack based upon the width and the length was completely based on the crack quantification model evaluation. Also, the integrated model as proposed by them has, crack length and change detection supported by neural networks to predict crack depth and 3-D visualization of crack patterns. Past researches developed a model that numerically represents the defects (21). Their integration model consists of crack quantification and detection, neural network, and 3-D visualization model respectively. Another study proposed an image analysis method to capture thin cracks and minimize the requirement for pen marking in reinforced concrete structural tests. They have used the studies like crack depth prediction, change in detection without image registration, crack

pattern recognition based on artificial neural networks, applications to micro-cracks of rocks, and efficient sub-pixel width measurement (22).

Another study has developed a fully automatic method to detect crack in the pavement images (23). They utilized a geodesic algorithm that eliminated the pavement shadows but kept the cracks. Then, by using the tensor voting methods, crack probability map were illustrated through a graph model. Finally, they derived Minimum Spanning Trees from which the crack extraction data can be taken off. Another study proposed a method in which concrete cracks were detected from 2D images of concrete surfaces by removing the noise from the image (24).

I addition, a new approach for automatically detecting crack defects with dark colors and low contrasts in magnetic tile images was proposed by (25). In their methodology, the original images were first decomposed and reconstructed based on the fast discrete curvelet transform (FDCT). Then the thresholds of decomposition coefficients were calculated by which the surface textures in the images can be removed. As an alternative to the previous methods, recently an study developed a non-contact vision-based fatigue crack detection technology, which is based on image overlapping (6). Moreover, like other non-contact technologies, their methodology has shorter deployment time, is more autonomous and economical in comparison with the traditional contact methods.

Using this information, the research team proposed the following technological advancement, which made use of AR tools for transportation infrastructure, and cracks in particular. The research team suggested that the inspectors' awareness of the damage could be improved by the application of AR headsets such as HoloLens. During the video recording, the images could be processed in real time, with the HoloLens computer capabilities. By using HoloLens, the inspectors would be able to detect cracks that could not be detected easily in real time otherwise. This solution, in turn, may provide the inspectors with an estimate damage assessment and damage prognosis of the structure. It also fulfilled the three major objectives of the research project: (1) it allows collecting objective data in the field faster and more reliably; (2) it permits registering bridge data that can be compared across time or across inspectors; and (3) it makes it possible to share the data from past inspections with the inspector. This research project focused on the computational tasks which were new and required specific programming understanding of both Unity and C#, but also the knowledge of the large amount of computer vision work developed by the community of Structural Health Monitoring (SHM) for crack detection using cameras. As a result, this project aimed to be a reference for researchers, practitioners, industry, and users interested to use AR for crack inspection.

## 3.2. AR for Infrastructure; Background Studies

In many science and engineering fields, visualization tools can improve the users' understanding of the environment, facilitates their interactive experience and promote information communication about a complex phenomenon. The visualization can also illustrate the potential application of an abstract concept for real world circumstances. A new branch of visualization that has been attracted the attention of engineering community is Virtual Reality (VR), which blocks the users' field of view, replaces the user's physical environment with an entirely virtual scene and takes the control of visual and hearing senses of users. However, reproduction of a viable accurate real engineering circumstance in virtual world for example tasks such as model engineering (the process of developing, editing, archiving, and maintaining 3D models), can be costly, laborious,

and hard to achieve (14). Contrary to VR, AR does not deduct the perception of the physical environment from users; instead, AR integrates the physical world with the digital objects of virtual environment (26).

AR has been conventionally known as the superimposition of digital or computer-generated content over the existing environment. AR is also defined as a technology that merges the virtual and physical components in the real world, in real-time, and in three dimensions (27). A wearable AR device helps and allows an onsite inspector to perform hands-free inspection tasks by superimposing the relevant information, such as technical drawings, previous inspection reports or history, manuals of specifications and standards, and holograms onto the real scene.

The engineering community started adopting AR in the 1960's (28). The preliminary experiences of the blend of real and virtual world, however, had several limitations including low resolution and brightness, short field of view, and lack of interactive features. In the next three decades, AR researchers focused on addressing visualization problems. In 1996, an AR system was developed that showed the location of columns behind a finished wall, the location of re-bars inside one of the columns, and performed structural analysis of the column (29). In 1999, a similar AR testbed system was used to address spaceframe construction (30). These systems focused on demonstrating the potential of AR's X-Ray vision with a lab-based approach. However, they were neither transferable to a construction job site nor could they be used for real-time on-site applications. Additionally, challenges related to occlusion were experienced with AR devices in 1990's. Occlusion, also known as obstruction, of real objects by virtual ones was not possible in conventional optical see-through displays. Such specific problem areas in AR displays have been overcome by more recent technical advancements.

Recent achievements have shown particular promise for collecting measurements. These advancements in AR technology have enabled use of AR to enhance infrastructural projects by simulating designed structures before their construction, providing virtual site visits, offering effective means for online interactions, and developing new teaching strategies (31). Additionally, these developments have facilitated the evaluation of dimensional and geometrical position of physical objects (32). For example, an AR camera (ARCam) has been successfully used to inspect the column anchor bolt positions before installing a steel column, and to assess its plumbness after installation. Figure 1 shows different applications of AR tools for infrastructure industry; particularly dimensional measurement with AR headsets for structural inspection is demonstrated in Figure 1.

The application of AR headsets for object detection using image processing is explored in previous studies. Additionally, the application of AR headsets for image-based crack detection and characterization is also evaluated in previous researches. For example, the use of AR technology for object detection was employed in several previous studies (33–38). Applying AR tools for crack identification and characterization is also, investigated in the earlier studies (12,39,40). Figure 2 presents the methodology of the mentioned studies. While the past studies have substantially enhanced our knowledge of AR systems for image-based object detection and characterization, because of the limited computational power available on AR headsets, they used a supplementary immobile computing device for processing their detection algorithms.
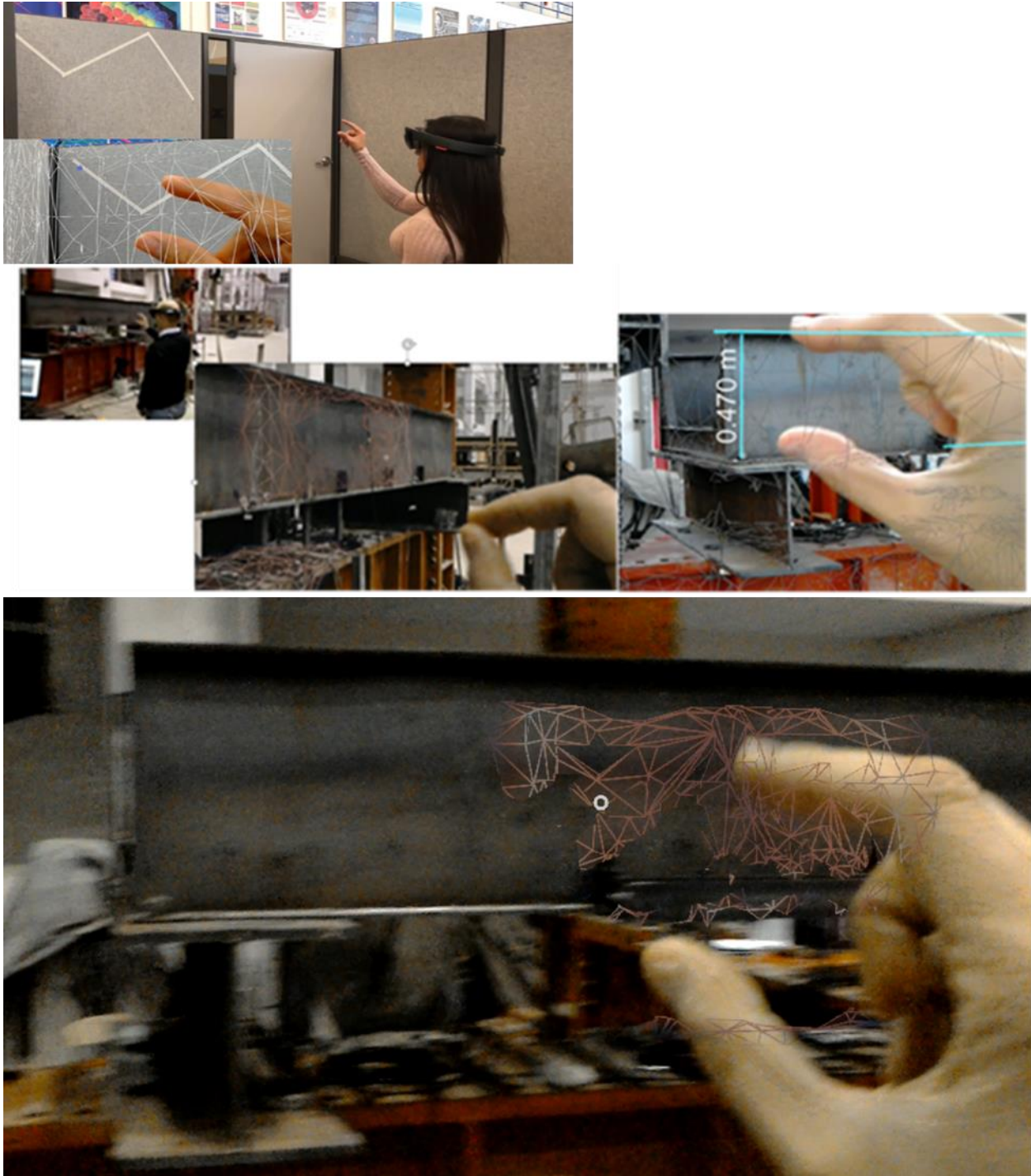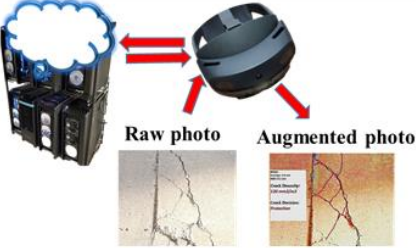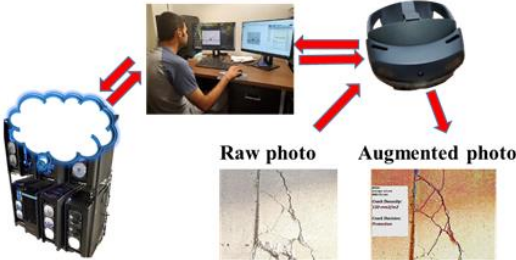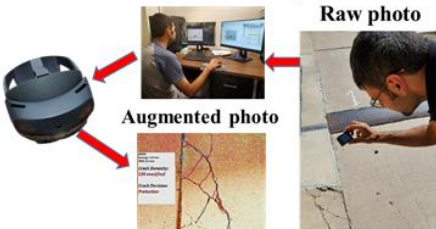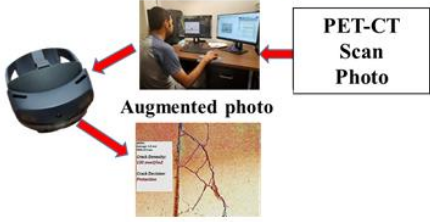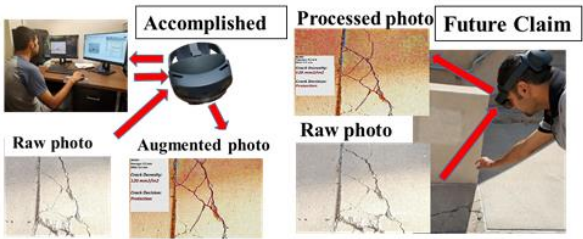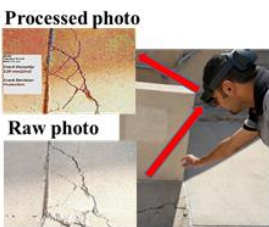
**Figure 1. Application of AR in infrastructure industry.**

| Publication | Required Connection between Hardware |
|:---:|:---:|
| (33,35,36,38,12) |  |
| (34) |  |
| (40) |  |
| (37) |  |
| (39) |  |
| Present study |  |

**Figure 2. Comparison of the past and the present image-processing methods.**

Figure 2 shows the types of hardware used in the previous methodologies and the connection that are needed to implement the methodologies. In addition, Figure 2 compares the hardware and the connection requirement of the past studies and this research. Figure 2 shows this methodology requires less hardware than the past studies. Additionally, while the past methodologies necessitates one or more connections between different devices, this research requires no connection for implementing crack detection and characterization.

# 4. METHODOLOGY

## 4.1. Detection System

The detection system was meant to improve the concrete inspection process in terms of accuracy, comfort and time by creating an application that shows potential cracks using real-time image to the inspector. This application contains the following main features:

- Receive real world image of concrete structure at real-time.

- Process the photo online.

- Mark any potential crack in the photo and show it to the inspector.

- Save the crack characteristic and image via photo or videos.

- Enabling the user to accurately detect and measure the cracks with the both hands free.

### 4.1.1. Required Software and Device

We used Microsoft HoloLens Mixed Reality (MR) Head Mounted Display (HMD) system (Figure 3) for implementing our crack extraction system. The HoloLens by Microsoft Corp. is the world's first standalone and untethered MR-HMD that possesses the unusual capability to perceive the space around it and thus maintaining a coordinate system which can be used to place objects, or holograms, in three dimensional space, directly in the user's field of view. (13).

There are other MR-HMD devices in the market; however, as far as the authors are aware of, they require a wired connection to an external computer and therefore, the user's limited motion of range will be caused by the necessity of a permanent connection to a computer. In addition, the other devices are only in sale for a comparatively short period. Therefore, it is hard to find scientific publications describing applications for them (41). Therefore, we found the Microsoft HoloLens device as the best possible means to our previously mentioned goals.



**Figure 3. The required device for employing the app.**

Unity and Microsoft Visual Studio software tools were employed for creating crack detection app. Unity is recommended by Microsoft, to create HoloLens applications using the UWP. The Mixed Reality Toolkit (MRTK), which is a cross-platform toolkit for building Mixed Reality experiences for AR were installed in Unity. Additionally, C Sharp was used as the programming language for creating the application.

### *4.4.2. Detection Algorithm*

We used Canny algorithm for crack detection. Canny detection is a technique to extract useful structural information from different vision objects and dramatically reduce the amount of data to be processed. It has been widely applied in various computer vision systems. It is a multi-stage algorithm and each stage has an especial function in the detection process. The process of Canny edge detection algorithm can be broken down to five different steps:

- Apply a smoothing filter to smooth the image in order to remove the noise

- Find the intensity gradients of the image

- Apply gradient magnitude thresholding or lower bound cut-off suppression to get rid of spurious response to edge detection

- Apply double threshold to determine potential edges

- Track edge by hysteresis: Finalize the detection of edges by suppressing all the other edges that are weak and not connected to strong edges.

Present project utilized luminosity method to convert an RGB image to a grayscale image as described in equation 1.

$$\text{Grayscale} = 0.299R + 0.587G + 0.114B \qquad [1]$$

where:

R =red level in RGB image;

G= grey level in RGB image;

B=blue level in RGB image.

Since the mathematics involved behind the scene are mainly based on derivatives (next step Gradient calculation), edge detection results are highly sensitive to image noise.

One way to get rid of the noise on an image, is by applying a blurring Kernel that smooth the image. To do so, image convolution technique is usually applied with a Gaussian Kernel (3x3, 5x5, 7x7 etc…). However, there exists the possibility of employing other smoothing filters and therefore a number of experiments were carried out using different blurring method as described in Table 1 and median filter were finally selected. The kernel size depends on the expected blurring effect. Basically, the smallest the kernel, the less visible is the blur. However, to reduce the processing time, we used a 3x3 Kernel in this project.

**Table 1. The performance of different filtering methods from the highest (5) to the lowest (1)**

| Filtering Method | Speed | Noise reduction performance | Edge preservation performance |
|---|---|---|---|
| Averaging | 4 | 1 | 1 |
| Median filter | 5 | 3 | 5 |
| Bilateral filter | 2 | 4 | 3 |
| Gaussian filter | 3 | 2 | 2 |
| Bilateral filter combine with Gaussian filter | 1 | 5 | 4 |

The Gradient calculation step detects the edge intensity and direction by calculating the gradient of the image using edge detection operators.

Edges correspond to a change of pixels' intensity. To detect it, the easiest way is to apply filters that highlight this intensity change in both directions: horizontal (x) and vertical (y).

When the image is smoothed, the derivatives Ix and Iy w.r.t. x and y are calculated. It can be implemented by convolving I with Sobel kernels Kx and Ky, respectively as shown in Figure 4:

| X – Direction Kernel | | |
|---|---|---|
| -1 | 0 | 1 |
| -2 | 0 | 2 |
| -1 | 0 | 1 |

| Y – Direction Kernel | | |
|---|---|---|
| -1 | -2 | -1 |
| 0 | 0 | 0 |
| 1 | 2 | 1 |

**Figure 4. The X-Y Kernels.**

Ideally, the final image should have thin edges. Thus, we must perform non-maximum suppression to thin out the edges. The principle is simple: the algorithm goes through all the points on the gradient intensity matrix and finds the pixels with the maximum value in the edge directions. The next step is double thresholding. The double threshold step aims at identifying 3 kinds of pixels: strong, weak, and non-relevant:

- Strong pixels are pixels that have an intensity so high that we are sure they contribute to the final edge.

- Weak pixels are pixels that have an intensity value that is not enough to be considered as strong ones, but yet not small enough to be considered as non-relevant for the edge detection.

- Other pixels are considered as non-relevant for the edge.

Now you can see what the double thresholds holds for:

- High threshold is used to identify the strong pixels (intensity higher than the high threshold)

- Low threshold is used to identify the non-relevant pixels (intensity lower than the low threshold)

- All pixels having intensity between both thresholds are flagged as weak and the Hysteresis mechanism (next step) will help us identify the ones that could be considered as strong and the ones that are considered as non-relevant (https://towardsdatascience.com).

Hough Line Transform algorithm can be employed to differentiate between cracks and the straight lines such as wall corners or concrete grooves as demonstrated in Figure 5. The Hough transform is a feature extraction technique used in image analysis, computer vision, and digital image processing. The purpose of the technique is to find imperfect instances of objects within a certain class of shapes by a voting procedure. In many cases, an edge detector (Canny algorithm in this project) can be used as a pre-processing stage to obtain image points or image pixels that are on

the desired curve in the image space. Due to imperfections in either the image data or the edge detector, however, there may be missing points or pixels on the desired curves as well as spatial deviations between the ideal line/circle/ellipse and the noisy edge points as they are obtained from the edge detector. For these reasons, it is often non-trivial to group the extracted edge features to an appropriate set of lines, circles or ellipses. The purpose of the Hough transform is to address this problem by making it possible to perform groupings of edge points into object candidates by performing an explicit voting procedure over a set of parameterized image objects (42).



**Figure 5. Crack vs concrete groove (https://www.concretenetwork.com).**

## 4.2. Measurement System

Our goal is to improve the concrete inspection process in terms of accuracy, comfort and time by creating an application that shows any potential cracks and their characteristic using 3D image to the inspector. This application contains the following main features:

- Mark any potential crack in real world using 3D images or 3D videos at real-time.

- Find the size and the width of the cracks during inspection.

- Show the size and the width of the cracks at real time.

- Save the crack characteristic and image via photo or videos.

- Enabling the user to accurately detect and measure the cracks with the both hands free.

### 4.2.1. Required Software and Device

As in section 4.1, We used Microsoft HoloLens Mixed Reality (MR) Head Mounted Display (HMD) system (Figure 1) for implementing our crack characterization system. The HoloLens is Microsoft's take on AR, which can be called mixed reality, using multiple sensors, advanced optics, and holographic processing that melds seamlessly with its environment. These holograms can be used to display information, blend with the real world, or even simulate a virtual world.

### 4.2.2. Crack Width Measurement Approach

Canny edge detection was used in present project for extracting the edges of cracks. Canny is a technique to extract useful structural information from different vision objects and dramatically reduce the amount of data to be processed. It has been widely applied in various computer

vision systems. Canny has found that the requirements for the application of edge detection on diverse vision systems are relatively similar. Thus, an edge detection solution to address these requirements can be implemented in a wide range of situations. The general criteria for edge detection include:

1. Detection of edge with low error rate, which means that the detection should accurately catch as many edges shown in the image as possible

2. The edge point detected from the operator should accurately localize on the center of the edge.

3. A given edge in the image should only be marked once, and where possible, image noise should not create false edges.

To satisfy these requirements Canny used the calculus of variations – a technique which finds the function which optimizes a given functional. The optimal function in Canny detector is described by the sum of four exponential terms, but it can be approximated by the first derivative of a Gaussian function. Among the edge detection methods developed so far, Canny edge detection algorithm is one of the most strictly defined methods that provides good and reliable detection. Owing to its optimality to meet with the three criteria for edge detection and the simplicity of process for implementation, it became one of the most popular algorithms for edge detection.

The schematic view of pixels between edges of cracks in x and y direction is shown in Figure 6. By applying Canny algorithm, the XY-coordinates of the edges of cracks and direction of gradient of the pixels in the edges of cracks were fully extracted. Then to measure the width of crack the number of pixels between two edges of crack is calculated.



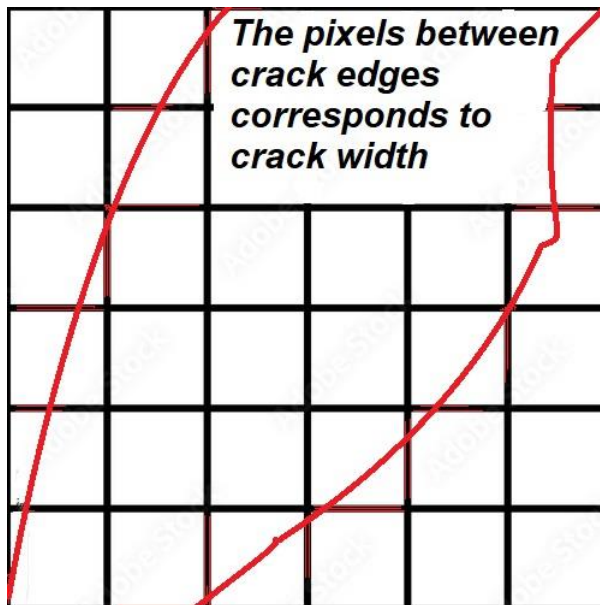**Figure 6. Schematic view of pixels between edges of cracks.**

We used "camera-To-World-Matrix" capability in unity to obtain the distance between the HoloLens camera and the target crack. This is a read-only matrix that transforms XYZ coordinates

from camera space to world space. This matrix shows where a HoloLens space point is in the world (in relation to a specific real-world reference point).

We calibrated the HoloLens app; holding the HoloLens at several distance to a reference object ($d_1, d_2... d_n$) and removed the measurement error at each distance. A schematic image of calibration process is shown in Figure 7.
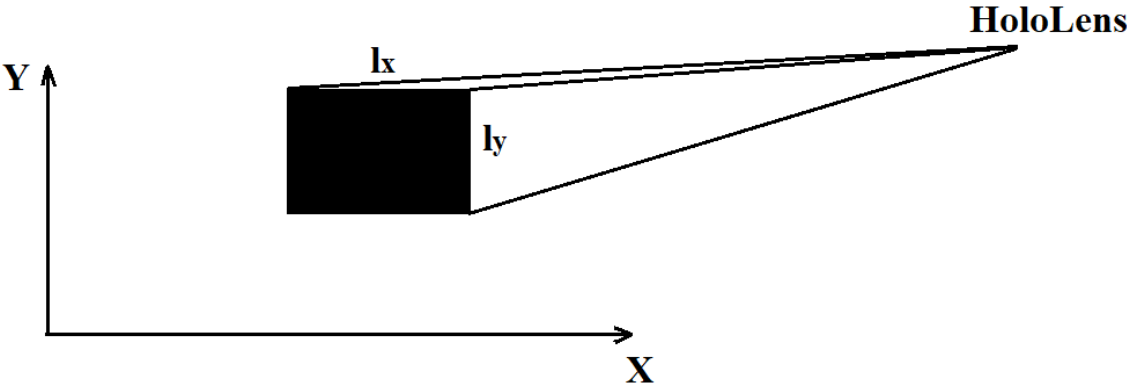


**Figure 7. The reference used in the calibration process.**

Finally, the pictures of measured portion of crack and the measurement results appears in front of the user in real-time as it is shown in Figure 8 for a real crack. The place of maximum crack thickness is overlaid by a line and shown to the HoloLens user.
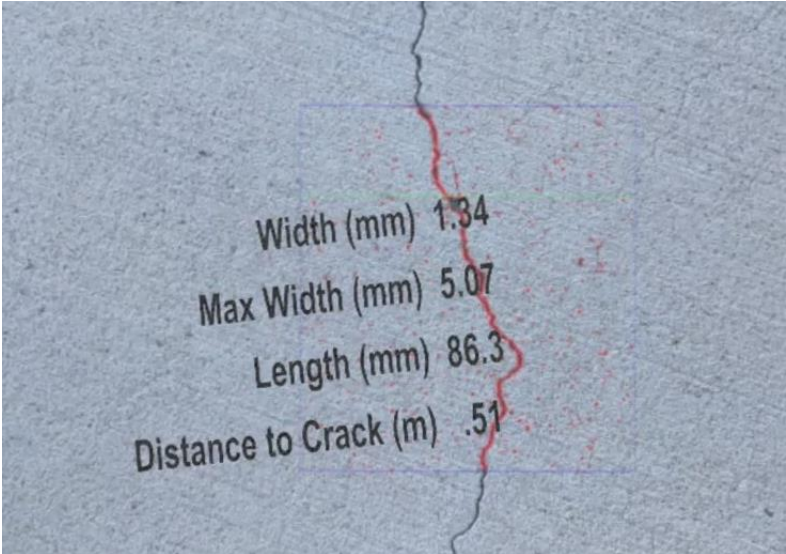


**Figure 8. The segmented HoloLens view in measuring app.**

# 5. ANALYSIS AND FINDINGS

## 5.1. Detection System Analysis

We used Microsoft HoloLens (Figure 1) to implement the code in realistic experiments that are similar to field applications that will be employed in the implementation phase. A repeated PhotoCapture or Webcam script produced the input photo and the photo was then processed inside the HoloLens. The processed photo finally appeared as a texture in front of the user as shown in Figure 9. The position of crack on the real object is instantly recognizable from the processed photo.
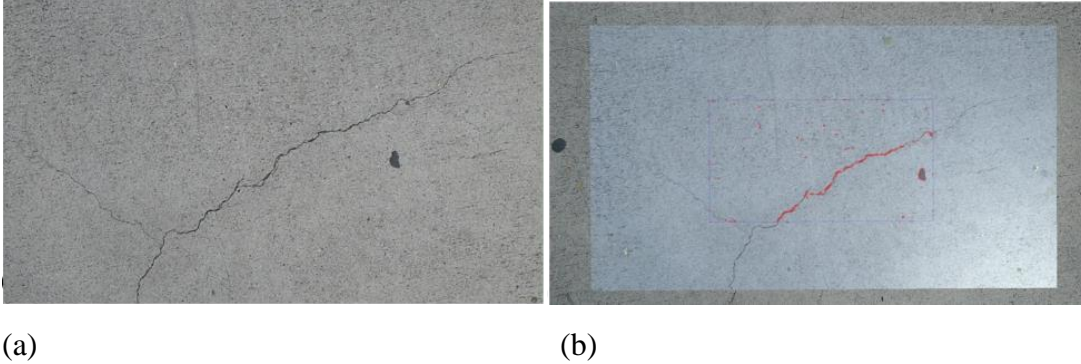


(a)                                                                                  (b)

**Figure 9. Crack detection experiment; a) unprocessed image b) the processed image showing the crack in front of the experiment operator.**

Figure 10 shows AR inspection of concrete pavement and compare it with the traditional visual inspection. Figure 10 (a) shows the inspection without AR headset cannot measure the crack without going through the time-consuming subjective process of manual measurement. The inspector in Figure 10 (b) can instantly characterize the crack with AR app and also save the crack information using AR capabilities. Additionally, the inspector in Figure 10 (c) can hardly observe and detect the tiny crack that can easily observed in using AR headset as shown in Figure 10 (d).

For the evaluation of the system in terms of accuracy Precision –Recall, the researchers conducted the following analysis. The analysis includes recall, precision and score:

- Recall is the percentage of reference data, which is explained by the extracted data, i.e., the percentage of true cracks that could be extracted by the filters. Recall $\epsilon$ [0;1] and its optimum value is 1.
- Precision represents the percentage of correctly extracted crack data, i.e., the percentage of extraction that matches the reference crack. Precision $\epsilon$ [0;1] and its optimum value is 1.
- Score is a more general measure of the final result combining Recall and Precision into a single measure. Score $\epsilon$ [0;1] and the optimum value is 1.

The formulas for the three indexes are listed below:

$$\text{Recall} = \frac{\text{length of matched reference}}{\text{length of reference}} = \frac{\text{Number of matched crack pixels of reference}}{\text{length of crack pixels of reference}} \quad [2]$$

$$\text{Precision} = \frac{\text{length of matched extraction}}{\text{length of extraction}} = \frac{\text{Number of matched crack pixels of extraction}}{\text{length of crack pixels of extraction}} \quad [3]$$

$$\text{Score} = \frac{2 \times \text{Recall} \times \text{Precision}}{\text{Recall} + \text{Precision}} = \frac{\text{Number of matched crack pixels of extraction}}{\text{length of crack pixels of extraction}} \qquad [4]$$



(a)                                   (b)



(c)                                   (d)

**Figure 10. Some of the pavement cracks at the University of New Mexico.**

## 5.1.1. Experiments: Phase I (Exploratory)

The researchers tested several real surface cracks of the concrete pavement with different width at the University of New Mexico at diverse times of day (under different lighting condition) to evaluate the tool in terms of accuracy. In the first step of experiments, we applied precision–recall analysis to 15 cracks which were detected by the HoloLens 1st generation device. We applied the

detection system to the cracks from different distances. However, if the application were not able to detect the majority of a crack during the experiments, we let the HoloLens to come as close as 600mm to the crack. This is approximately the worst-case-scenario for visual inspection distance in several codes and standards. For example, ASME BPVC- Section IX (T-952) for visual inspection obligate the inspectors to place their eye within 24 in. (610 mm) of the surface to be examined. By applying the crack detection HoloLens app to different patterns of real cracks, marked red curves in the positions of cracks will be appear as illustrated in Figure 11 for different crack patterns. Processed and unprocessed photos for longitudinal crack, traverse crack, craze crack, corner crack, D- crack, diagonal crack, and map crack are demonstrated in Figure 11 (a) to (g), respectively. Figure 11 shows that the AR app can detect the cracks of different patterns and shapes.



(a)

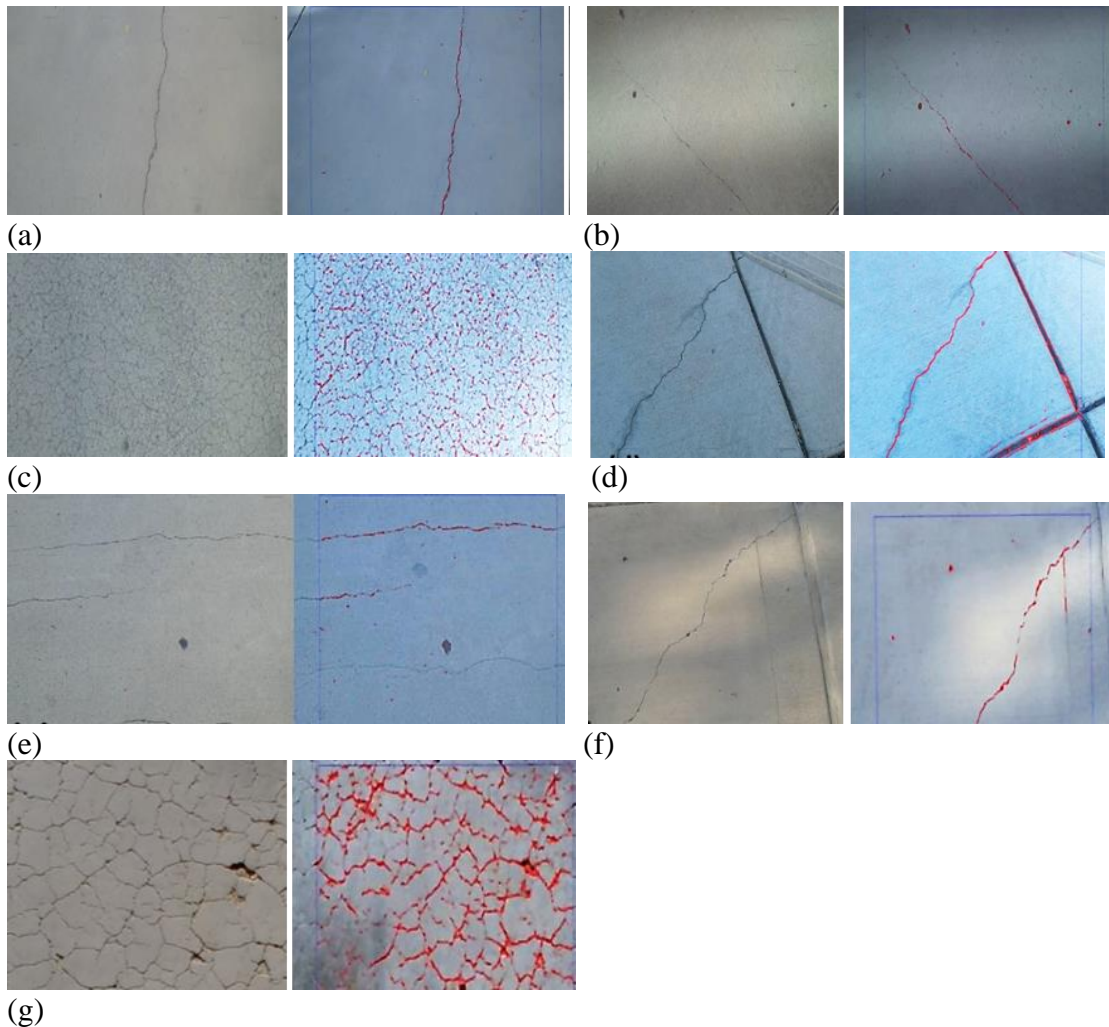(b)

(c)

(d)

(e)

(f)

(g)

**Figure 11. Resulting photos for different types of cracks a) longitudinal crack, b) traverse crack, c) craze crack, d) corner crack, e) D- crack, f) diagonal crack, g) map crack.**

The result of the first set of experiments is shown in Figure 12. It is seen from Figure 12 that the average of recalls for all 15 experiments is 0.75 meaning that typically, 75 percent of the surfaces of the cracks in each experiment were truly detected by the HoloLens tool and were shown to the

inspector. The average precision for the experiments is 0.69 that shows 69 percent of the predictions were correctly a part of a crack and 31 percent of the predictions were false.

Canny algorithm, as an edge detection algorithm, showed sensitivity to non-crack edges such as the grooves in concrete pavement and the presence of these edges resulted in an increase in the false positive predictions, which in turn, reduced the Precisions for these edges. Therefore, the fact that the cracks (13), (14) and (15) of Figure 12-panel a, are adjacent to pavement groves, can explain why their Precisions are much less than the average of the Precisions.

In addition, the wider and closer cracks to HoloLens were detected by the system easier than the smaller and further cracks that appear less contrasted. For example, the lower Recall values of crack (12) of Figure 12-panel a, is due to its relatively far distance to the HoloLens compared to the other cracks. For selecting the efficient thresholds of Canny algorithm in this part, several experiments were performed, in which we aimed at removing the sensitivity of the HoloLens application to shadows and surface irregularities. Therefore, the existence of shadow does not cause a meaningful inaccuracy in the quality measures as shown in Figure 12-panel c. However, as Figure 12-panel c reiterates, Precisions when there are non-crack edges near the cracks are lower in value than when the cracks are far away from the non-crack edges.

The authors found no data related to online crack detection with ARSG in the literature; therefore, no comparison of the achieved quality measures is drawn in this section. The method might seem less accurate than some of the past novel crack detection methods with computer such as (23,43) that achieved higher quality measures. It should, however, be noted that the detection approach employed in present project, which tried to provide an assisting means to increase the visual inspection capability of inspectors, is different from the methodologies in the mentioned studies that introduced different substitutes for visual inspection.

The average of recalls for all 15 experiments is 0.75 that means typically, 75 percent of the surfaces of the cracks in each experiment were truly detected by the HoloLens tool and were shown to the inspector. The claim is that, because of the real-time nature of the proposed system, when a considerable part of a crack is shown to a human inspector during visual inspection process, this means that the inspector have noticed the crack and can make their professional judgment about it. The other advantage of the HoloLens application is that the inspector can detect the cracks if they are distant or in a hard to access location. The ARSG is able to augment the PhotoCapture in these conditions and the inspectors can perform their evaluation using the augmented HoloLens PhotoCapture and without needing any access tools such as a snooper truck or ladder. Furthermore, the system provides the possibility of simultaneous supervision of the inspection process by an office supervisor via HoloLens livestream, which is the ARSG capability to share what the user is eying at real-time. Therefore, the proposed crack detection system has the capacity to facilitate the visual inspection process and it has the potential to make the inspection process much more accurate.
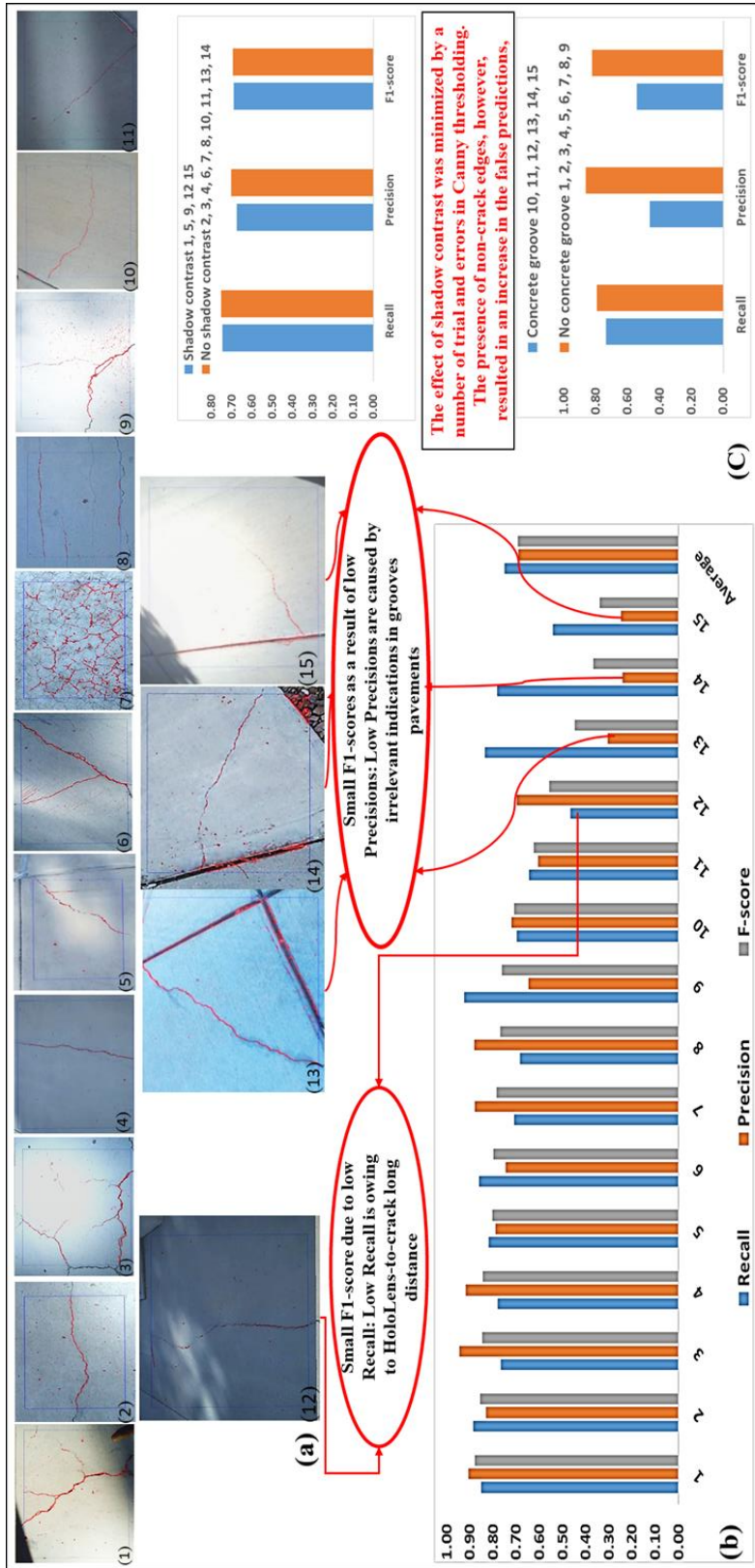
**Figure 12. Results of the precision-recall analysis for 15 cracks of the first experiment.**

### 5.1.2. Experiments: Phase II (Validation)

To evaluate the effect of effective parameters on the tool accuracy, several effective factors in AR systems such as the device position in relation to target object, the ARSG generation and processing power, camera mode and camera resolution were tested in the second step of experiments. In these experiments, four cracks with different average width (approximately from 0.5mm to 2,2mm) were chosen and examined by both 1$^{st}$ and 2$^{nd}$ generations of Microsoft HoloLens glasses from three different distances. Thresholds of Canny algorithm were same for both generation of ARSG and the cracks' width measured manually using a calibrated digital caliper with the resolution of 0.01mm. The stand used to hold the ARSG at fixed distances from the cracks and the tested cracks in the experiments, are described in Figure 13-panel a and b, respectively.
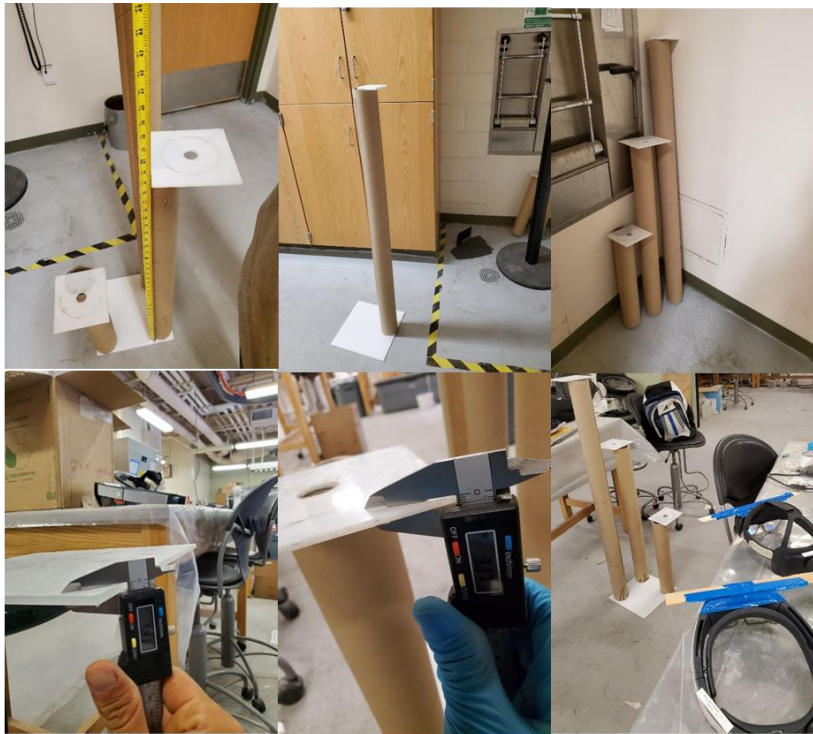


(a)



(b)

**Figure 13. The second experiments description (a) the description of the stand used to hold the ARSG at fixed distances from the cracks (b) the tested cracks characteristics.**

Figure 14 shows two consecutive sequence of the experiment (processed and unprocessed photo) for the four tested cracks.



(a)                                                    (b)

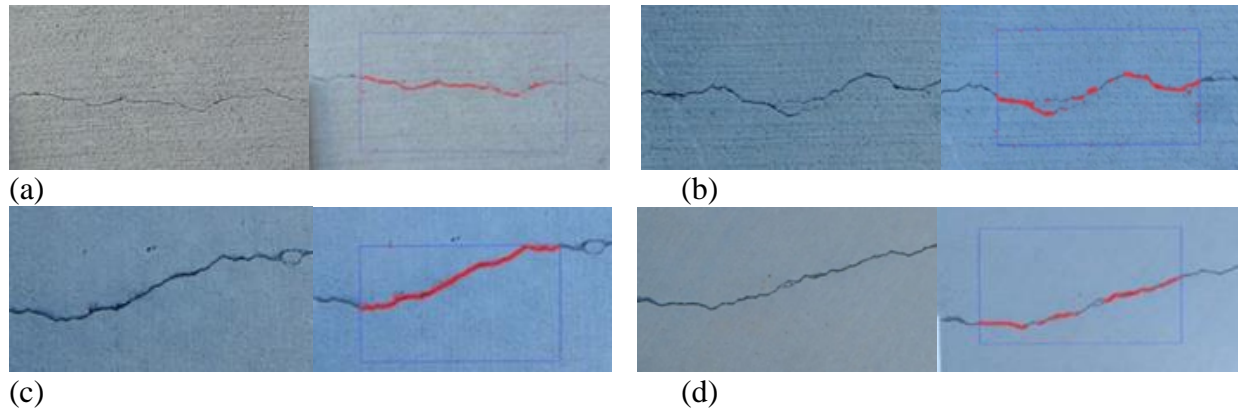(c)                                                    (d)

**Figure 14. Processed and unprocessed photo for the four tested cracks with width of (a) 0.6 mm (b) 1.1 mm (c) 1.6 mm, and (d) 2.4 mm, respectively.**

The two generations of ARSG is compared in Table 2.

**Table 2. Features and spec of 1st and 2nd generation of HoloLens.**

|  | **HoloLens2** | **HoloLens1** |
|---|---|---|
| **CPU Model** | QC Snapdragon 850 | Intel Atom x5-Z8100P |
| **CPU Cores** | 8 | 4 |
| **Memory** | 4GB | 1GB |
| **Storage** | 64 GB | 64 GB |
| **HPU** | 2nd Gen custom | 1st Gen custom |
| **Wifi** | Wifi 5 | 802.11ac |
| **Hand tracking** | both hands | one hand |
| **Eye-tracking** | Yes | No |
| **Field of view (FOV)** | 52° | 34° |
| **Weight** | 566 grams | 579 grams |
| **IPD adjustment** | Yes | Yes |
| **Display resolution** | 2048 × 1080 px (per eye) | 1280×720 (per eye) |

The first version of detection system with unmodified Canny algorithm was implemented in the Microsoft HoloLens and the processing time was calculated 68s for HoloLens1 which was far from a real-time system. However, after imposing two modifications in the algorithm, the processing time reduced to 0.8sec which is considered real-time in several past studies. These modifications and the resulting reduction in the processing time is described in Figure 15.

| Options | 1st Modification of Section 2.3 | 2nd Modification of Section 2.3 | Camera Mode | 1st Generation Processing Time | 2nd Generation Processing Time |
|---|---|---|---|---|---|
| A | Not used | Not used | Photo Capture | 68 Sec | t>1000 Sec |
| B | Not used | Not used | Webcam | Not Working | Not Working |
| C | Used | Not used | Photo Capture | Varies Depending on the Rectangle Size | Varies Depending on the Rectangle Size |
| D | Used | Not used | Webcam | Varies Depending on the Rectangle Size | Varies Depending on the Rectangle Size |
| E | Used | Not used | Photo Capture | 2.5 Sec | 4.8 Sec |
| F | Used | Not used | Webcam | Not Working | Not Working |
| G | Used | Used | Photo Capture | | 3.1 Sec |
| H | Used | Used | Webcam | 0.9 Sec | 0.8 Sec |

**Figure 15. The effect of code streamlining on the processing time.**

The results of these experiments describe the direction of change in crack quality measures based on different effective parameters as illustrated in Figures 16-17.

Figure 16 and 15 demonstrates that while the crack width, ARSG position and ARSG version have a high level of influence on accuracy, ARSG camera mood had a minimal effect on the image processing. Our results indicated that all quality measures constantly increases as crack width increases. The Recall and Score constantly decrease when ARSG's distance from the crack increases while Precision enhances with an increase in ARSG's distance. 2$^{nd}$ generation of HoloLens achieved bigger Recall than the 1$^{st}$ generation while the 1$^{st}$ generation superseded the 2$^{nd}$ generation in Precision. Overall, because the Score, which is the weighted average of Recall and Precision, is greater for HoloLens 2, the better performance for crack detection can be achieved with the newer version of the device.

Finally, it should be mentioned that the unclear HoloLens view in direct sunlight and price of the ARSG should be noted as the major limitations for implementing the current methodology for real-world application.
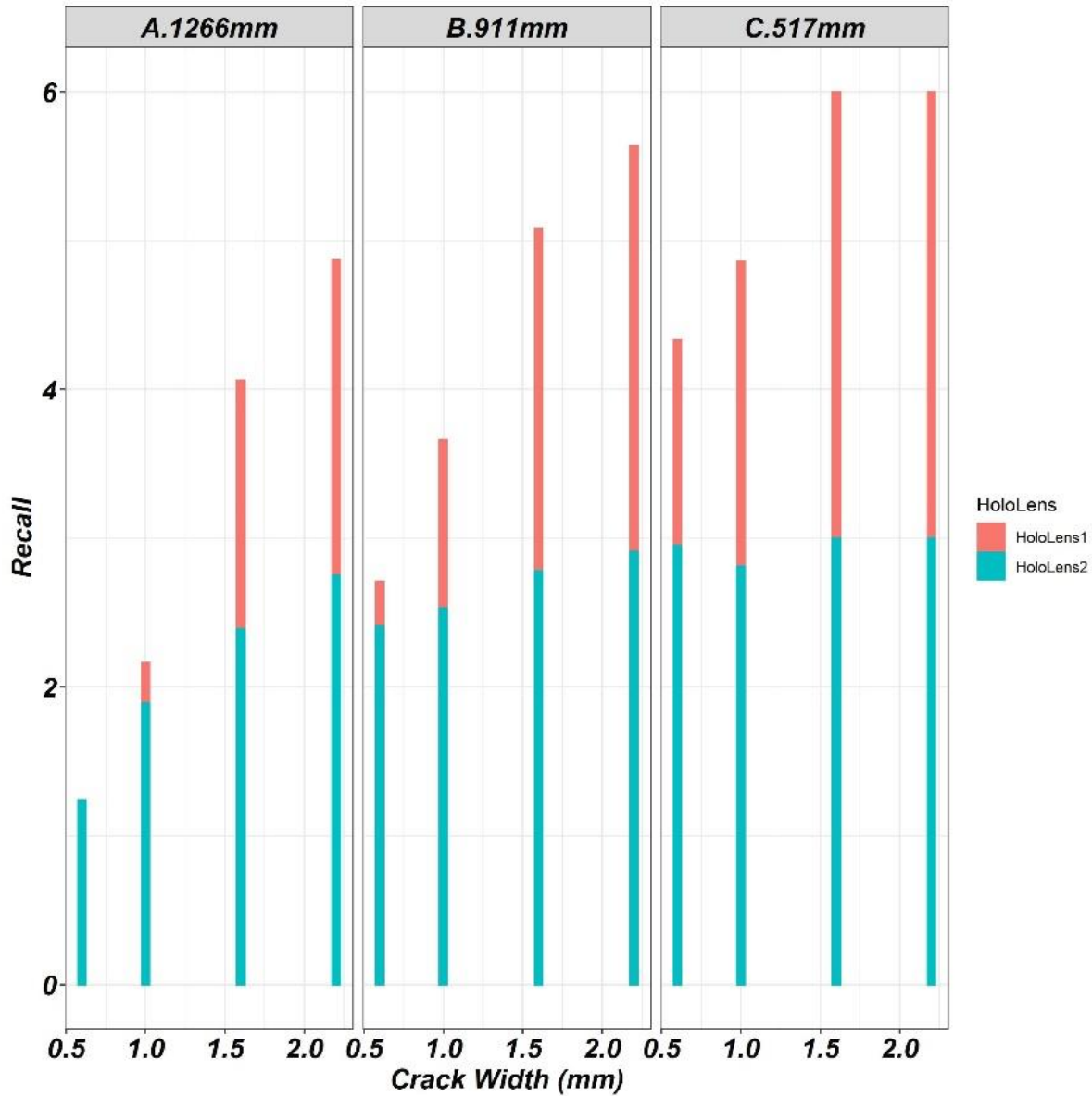
**Figure 16. The effect of crack-width, HoloLens Version, and HoloLens position on quality measures.**

## 5.2. Measurement System Analysis

The measurement application was put to test through a number of experiments using the pictures of cracks and real cracks. The following section will present these measurement experiments in two parts i.e. the crack picture experience and the real crack experience.
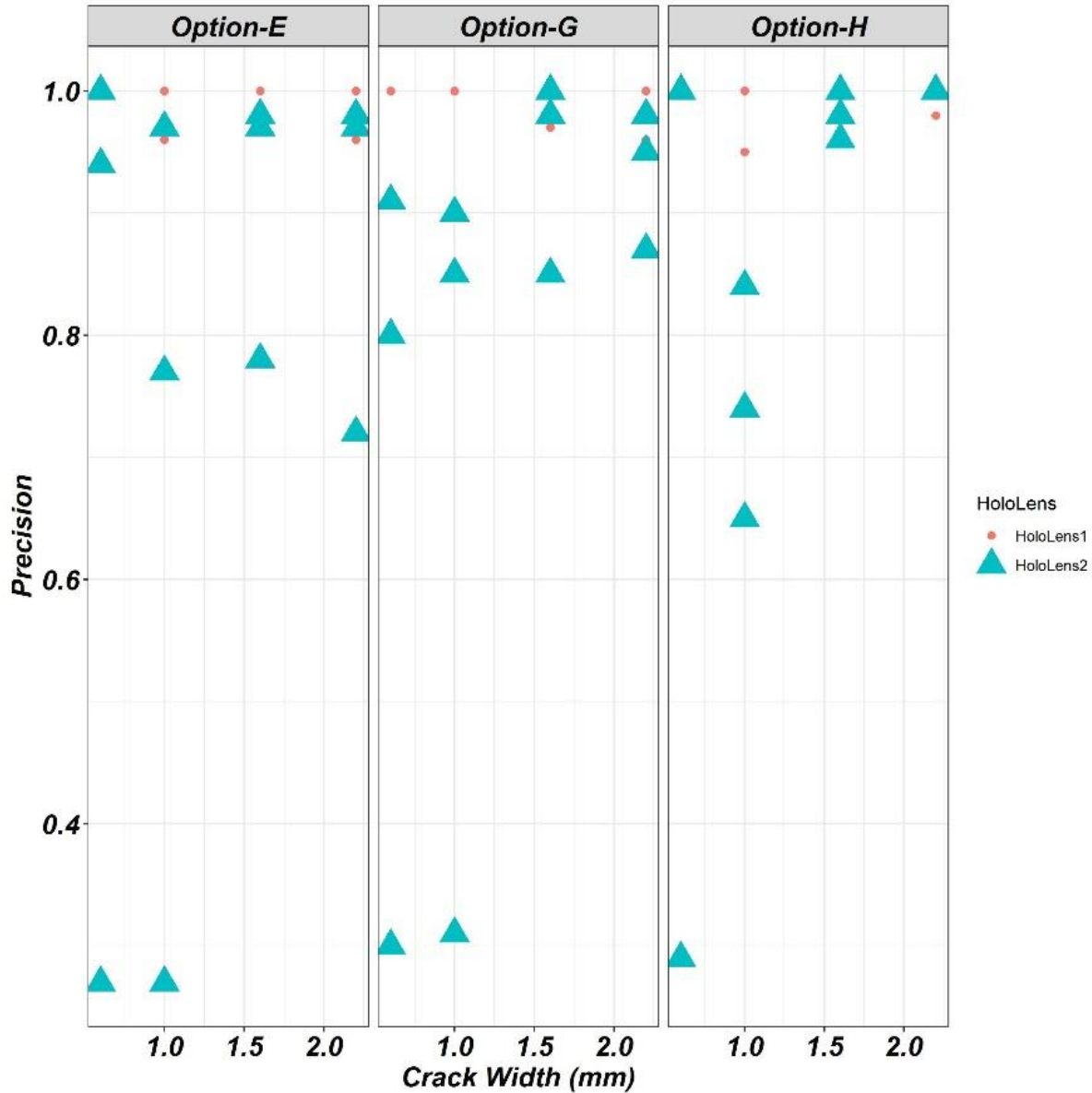
**Figure 17. The effect of crack-width, camera mood, algorithm modifications, and HoloLens position on quality measures.**
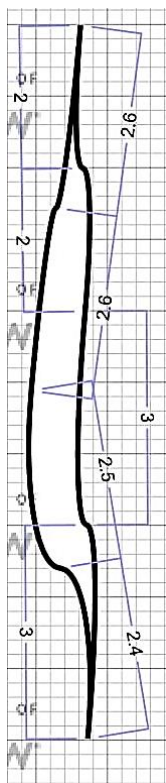
### 5.2.1. Crack Picture Experiments

In this part, we explored the accuracy of the application for the picture of three cracks of Figure 18 according to two statistical criteria including mean error and max error.

The manual measurement, app reading and the errors in the app reading for the image of Figure 18 are illustrated in Table 3. Both values of the maximum and average thickness of the cracks' image of Figure 18 are presented in Table 3. For this experiment, we run the app using the webcam texture code and with camera placed at 25 cm to the images (the distance at which calibration is carried out). We ignored the fluctuations in reading and used the median value of reading as the app readings.

From Table 3 the maximum error in a measurement is limited to 13.3 percent in both average and maximum measurement and corresponds to the crack c in Figure 18.

**Table 3. Cracks' picture thickness measurements.**

| Thickness(mm) | (a) Average | (a) Max | (b) Average | (b) Max | (c) Average | (c) Max |
|---|---|---|---|---|---|---|
| Manual Measurements (mm) | 4.5 | 7.5 | 4.5 | 7 | 4.5 | 10 |
| App Reading (mm) | 4.7 | 6.7 | 4.6 | 6.7 | 5.1 | 8.7 |
| Error | 0.2 | 0.8 | 0.1 | 0.3 | 0.6 | 1.3 |
| Percent Error | 4.4 | 10.7 | 2.2 | 4.5 | 13.3 | 13.0 |
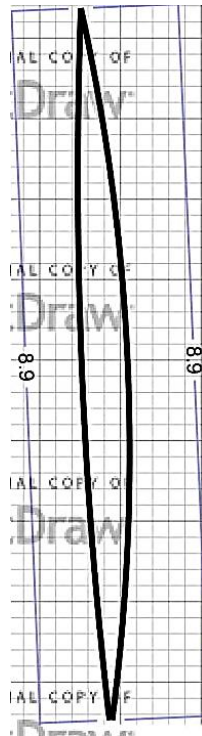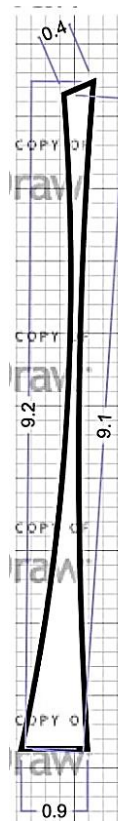


(a)                    (b)                    (c)

**Figure 18. Fake crack sketches.**

28

## 5.2.2. Crack Picture Experiments

In this part, the cracks on 5 concrete cylinder available at the Structural Laboratory at the University of New Mexico was manually measured using a digital caliper (Figure 19) and then these manual measurements were compared with the values of the app reading (Figure 20).
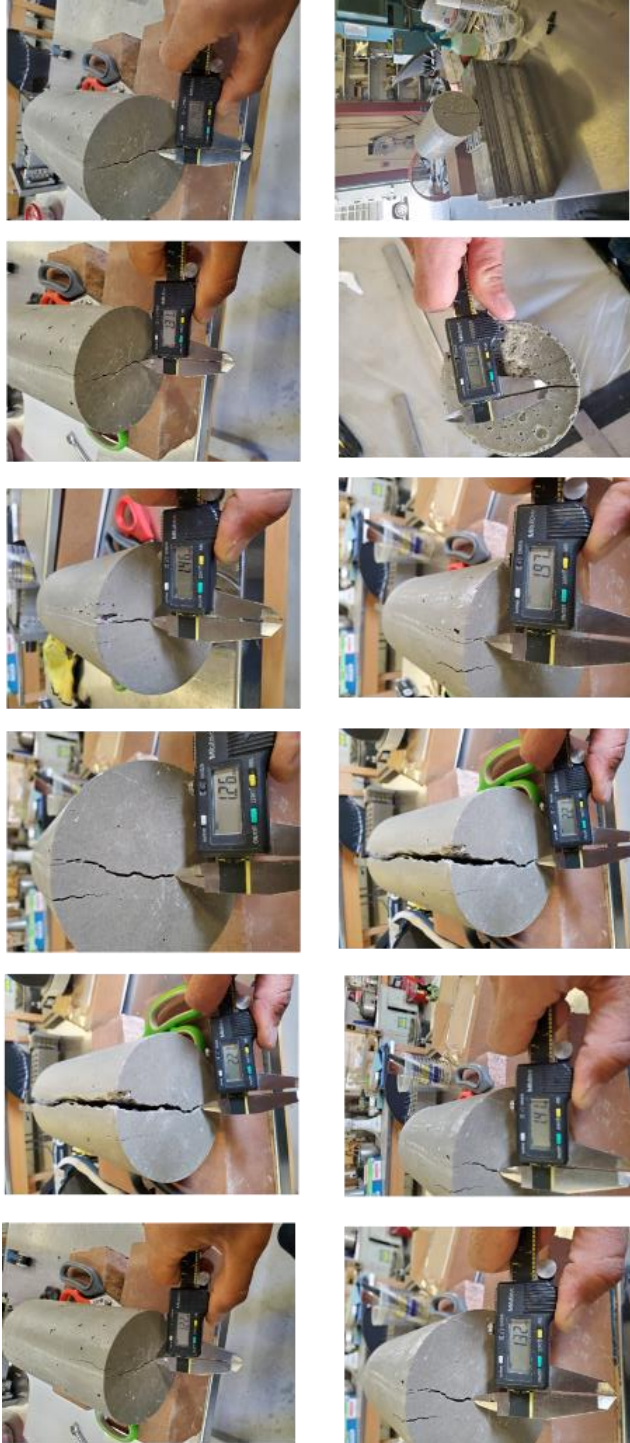


**Figure 19.Manual measurement of 5 cracked cylinder in real crack measurement experiments.**
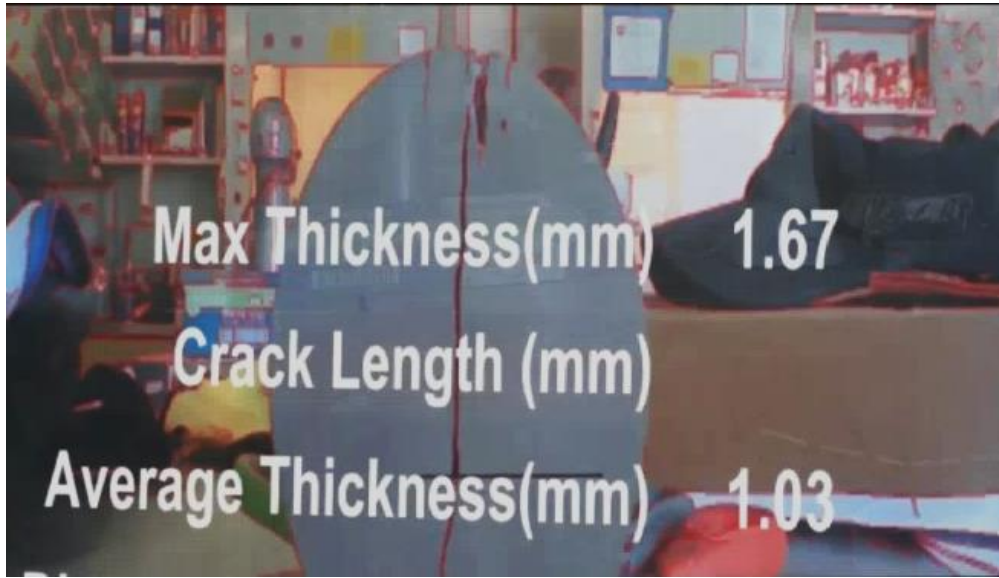
**Figure 20. App reading of 5 cracked cylinder in real crack measurement experiments.**

Table 4 evaluates the app measurement according to two statistical criteria including mean error and max error. From  Table 4 the maximum error in a measurement is limited to 16.7 percent in average thickness and 10 percent maximum measurement and both correspond to the narrowest tested crack.

**Table 4. The real crack thickness measurement.**

| Crack | Caliper (mm) | Caliper (mm) | App (mm) | App (mm) | Error% | Error% |
|---|---|---|---|---|---|---|
| No. | Average Thickness | Maximum Thickness | Average Thickness | Maximum Thickness | Average Thickness | Maximum Thickness |
| 1 | 1.2 | 2.0 | 1.0 | 1.8 | 16.7 | 10 |
| 2 | 1.8 | 2.5 | 1.6 | 2.7 | 11.1 | 8 |
| 3 | 2.1 | 3.2 | 2.3 | 3.3 | 8.7 | 3.1 |
| 4 | 3.4 | 4.5 | 3.5 | 4.1 | 3.0 | 8.5 |
| 5 | 4.2 | 7.6 | 3.8 | 7.0 | 9.5 | 7.9 |

# 6. CONCLUSIONS

This project report summarizes the work conducted to develop a novel framework for crack detection and crack evaluation in transportation structures using a combination of image-processing based tool and AR. The main emphasis of the work conducted in this project has been a practical tool that innovates the current limitations on AR outlined by industry, as well as a new method where the inspector can wear the headset and use AI to see cracks on real time in front of them. Both strengths and weaknesses of this implementation were addressed and the accuracy of the approach was evaluated using different experiment. The findings of this work show the promise of using a combination of image-processing and AR as a useful framework for facilitating the inspection process for transportation infrastructure stakeholders, including various sectors such as NMDOT, CN, LAC, and other owners like the city of Albuquerque and the UNM campus. The results showed that the AR application is of interest to both owners and industry. The feedback from industry has indicated that the AR application needs to be easier to use based on engineers testing the application and providing their feedback to the research team. The indication of the results of this work is encouraging in the technical level, but we believe further simplification in the human-AR interface needs to be added so bridge inspectors feel comfortable with the technical new capability and they use it eventually without supervision, which would be our goal.

To advance this AR in the implementation phase, the image-processing assisted AR inspection framework presented will be developed in the following new directions. First, a more comprehensive method for crack detection will be proposed so that the probability of detected edges to be crack will be given by application to the user, which has been a feature of interest to the owners and users to date and would be of value for higher trust in the application. Second, it was indicated by industry that they would be interested if AR would be able to find more defect types automatically.

A final conclusion from both results and recommendations from industry is that even AR has been developed to date to assist in automatic inspection of features, cracks, and defects, more work on human-machine interface and human-infrastructure interface needs to be advanced, including teaming with experts in human factors, psychology, cognition, workforce development, and technology-human frontiers.

# REFERENCES

1. FENVES SJ. Artificial intelligence-based methods for infrastructure evaluation and repair. Ann NY Acad Sci. 1984;431:182–93.

2. Stent S, Gherardi R, Stenger B, Soga K, Cipolla R. Visual change detection on tunnel linings. Machine Vision and Applications. 2016;27(3):319–30.

3. Phares B, Rolander D, Graybeal B, Washer G. Reliability of Visual Bridge Inspection. Public Roads. 2001;64:22–9.

4. Li Q, Shi Z, Zhang H, Tan Y, Ren S, Dai P, et al. A cyber-enabled visual inspection system for rail corrugation. Future Generation Computer Systems. 2018; 79:374–82.

5. Zhao Y, Roddis WMK. Fatigue Prone Steel Bridge Details: Investigation and Recommended Repairs. 2004; 1321358

6. Kong X, Li J. Non-contact fatigue crack detection in civil infrastructure through image overlapping and crack breathing sensing. Automation in Construction. 2019; 99:125–39.

7. Graybeal BA, Phares BM, Rolander DD, Moore M, Washer G. Visual Inspection of Highway Bridges. Journal of Nondestructive Evaluation. 2002;21(3):67–83.

8. ISO 4179:2005.

9. ACI Committee 224. 224R-01: Control of Cracking in Concrete Structures (Reapproved 2008).

10. Boresi AP, RJ. Advanced Mechanics of Materials. 6th edition. New York: Wiley; 2002; 681.

11. Yao Y, Tung S-TE, Glisic B. Crack detection and characterization techniques—An overview. Structural Control and Health Monitoring. 2014;21(12):1387–413.

12. Karaaslan E, Bagci U, Catbas FN. Artificial Intelligence Assisted Infrastructure Assessment using Mixed Reality Systems. Transportation Research Record. 2019;2673(12):413–24.

13. Wang S, Sakib Ashraf Zargar,, Fuh-Gwo Yuan 202. Augmented reality for enhanced visual inspection through knowledge-based deep learning. 2020.

14. Brooks WSM, Lamb DA, Irvine SJC. IR Reflectance Imaging for Crystalline Si Solar Cell Crack Detection. IEEE Journal of Photovoltaics. 2015;5(5):1271–5.

15. Pei C, Qiu J, Liu H, Chen Z. Simulation of surface cracks measurement in first walls by laser spot array thermography. Fusion Engineering and Design. 2016;109–111:1237–41.

16. Yeum CM, Dyke SJ. Vision-Based Automated Crack Detection for Bridge Inspection. Computer-Aided Civil and Infrastructure Engineering. 2015;30(10):759–70.

17. Gong C, Ding W, Mosalam KM, Günay S, Soga K. Comparison of the structural behavior of reinforced concrete and steel fiber reinforced concrete tunnel segmental joints. Tunnelling and Underground Space Technology. 2017;68:38–57.

18. Yu S-N, Jang J-H, Han C-S. Auto inspection system using a mobile robot for detecting concrete cracks in a tunnel. Automation in Construction. 2007;16(3):255–61.

19. Menendez E, Victores JG, Montero R, Martínez S, Balaguer C. Tunnel structural inspection and assessment using an autonomous robotic system. Automation in Construction. 2018;87:117–26.

20. Brown M, Lowe DG. Automatic Panoramic Image Stitching using Invariant Features. Int J Comput Vision. 2007;74(1):59–73.

21. Adhikari RS, Moselhi O, Bagchi A. Image-based retrieval of concrete crack properties for bridge inspection. Automation in Construction. 2014;39:180–94.

22. Yang Y-S, Yang C-M, Huang C-W. Thin crack observation in a reinforced concrete bridge pier test using image processing and analysis. Advances in Engineering Software. 2015;83:99–108.

23. Zou Q, Cao Y, Li Q, Mao Q, Wang S. CrackTree: Automatic crack detection from pavement images. Pattern Recognition Letters. 2012;33(3):227–38.

24. Nguyen HT, Won CS. Video retargeting based on group of frames. JEI. 2013;22(2):023023.

25. Li X, Jiang H, Yin G. Detection of surface crack defects on ferrite magnetic tile. NDT & E International. 2014;62:6–13.

26. Maharjan D, Agüero M, Mascarenas D, Fierro R, Moreu F. Enabling human–infrastructure interfaces for inspection using augmented reality. Structural Health Monitoring. 2021;20(4):1980–96.

27. Azuma RT. A Survey of Augmented Reality. Presence: Teleoperators and Virtual Environments. 1997;6(4):355–85.

28. Sutherland IE. A head-mounted three dimensional display. In: Proceedings of the December 9-11, 1968, fall joint computer conference, part I [Internet]. New York, NY, USA: Association for Computing Machinery; 1968 [cited 2021 Dec 21]. p. 757–64. (AFIPS '68 (Fall, part I)).

29. Webster A, Feiner S, MacIntyre B, Massie W, Krueger T. Augmented Reality in Architectural Construction, Inspection, and Renovation. undefined [Internet]. 1996

30. Mascareñas DD, Ballor JP, McClain OL, Mellor MA, Shen C-Y, Bleck B, et al. Augmented reality for next generation infrastructure inspections. Structural Health Monitoring. 2021;20(4):1957–79.

31. Behzadan AH, Dong S, Kamat VR. Augmented reality visualization: A review of civil infrastructure system applications. Advanced Engineering Informatics. 2015;29(2):252–67.

32. Shin DH, Dunston PS. Evaluation of Augmented Reality in steel column inspection. Automation in Construction. 2009;18(2):118–29.

33. Bahri H, Krčmařík D, Kočí J. Accurate Object Detection System on HoloLens Using YOLO Algorithm. In: 2019 International Conference on Control, Artificial Intelligence, Robotics Optimization (ICCAIRO). 2019. 219–24.

34. Corneli A, Naticchia B, Cabonari A, Boschê F. Augmented Reality and Deep Learning towards the Management of Secondary Building Assets. ISARC Proceedings. 2019;332–9.

35. Farasin A, Peciarolo F, Grangetto M, Gianaria E, Garza P. Real-time Object Detection and Tracking in Mixed Reality using Microsoft HoloLens: In: Proceedings of the 15th International Joint Conference on Computer Vision, Imaging and Computer Graphics Theory and Applications 2.020;165–72.

36. Liu L, Li H, Gruteser M. Edge Assisted Real-time Object Detection for Mobile Augmented Reality. In: The 25th Annual International Conference on Mobile Computing and

Networking [Internet]. New York, NY, USA: Association for Computing Machinery. 2019; 1–16.

37. Pepe A, Trotta GF, Gsaxner C, Wallner J, Egger J, Schmalstieg D, et al. Pattern Recognition and Mixed Reality for Computer-Aided Maxillofacial Surgery and Oncological Assessment. In: 2018 11th Biomedical Engineering International Conference (BMEiCON). 2018; 1–5.

38. Wang S, Guo R, Wang H, Ma Y, Zong Z. Manufacture Assembly Fault Detection Method based on Deep Learning and Mixed Reality. In: 2018 IEEE International Conference on Information and Automation (ICIA). 2018; 808–13.

39. Wang S, Zargar SA, Yuan F-G. Augmented reality for enhanced visual inspection through knowledge-based deep learning. Structural Health Monitoring. 2021;20(1):426–42.

40. Yamaguchi T, Shibuya T, Kanda M, Yasojima A. Crack Inspection Support System for Concrete Structures Using Head Mounted Display in Mixed Reality Space. In: 2019 58th Annual Conference of the Society of Instrument and Control Engineers of Japan (SICE). 2019; 791–6.

41. Lang S, Dastagir Kota MSS, Weigert D, Behrendt F. Mixed reality in production and logistics: Discussing the application potentials of Microsoft HoloLensTM. Procedia Computer Science. 2019;149:118–29.

42. Shapiro LG, Stockman GC. Computer Vision. 1st edition. Upper Saddle River, NJ: Pearson; 2001; 608.

43. Iyer S, Sinha SK. A robust approach for automatic detection and segmentation of cracks in underground pipeline images. Image and Vision Computing. 2005;23(10):921–33.